ARTICLE IN PRESS

Available online at www.sciencedirect.com

SCIENCE DIRECT®

ELSEVIER

Catalysis Communications 7 (2006) 281–284

CATALYSIS COMMUNICATIONS

www.elsevier.com/locate/catcom

Vapor phase synthesis of supported Pd, Au, and unsupported bimetallic nanoparticle catalysts for CO oxidation

Yonglai Yang [a], Khaled M. Saoud [a], Victor Abdelsayed [a], Garry Glaspell [a], Sarojini Deevi [b], M. Samy El-Shall [a,*]

[a] *Department of Chemistry, Virginia Commonwealth University, 1001 W. Main Street, Richmond, VA 23284-2006, United States*
[b] *Philip Morris USA Research Center, Richmond, VA 23234, United States*

Received 29 July 2005; received in revised form 2 November 2005; accepted 9 November 2005

Abstract

We report the vapor phase synthesis and characterization of supported Pd, Au and unsupported bimetallic nanoparticle catalysts for CO oxidation. The approach utilized in the present work is based on the laser vaporization/controlled condensation technique which uniquely combines the features of pulsed laser vaporization with the controlled condensation process from the vapor phase to synthesize nanoparticle catalysts of controlled size and composition. The results indicate that supported Pd/CeO_2, Au/CeO_2, and unsupported bimetallic CuPd, CuAu, and AuPd nanoparticle catalysts exhibit excellent activity for CO oxidation. The significance of the current method lies mainly in its simplicity, flexibility and the control of the different factors that determine the activity of the nanoparticle catalysts.

Recent advances in the synthesis and characterization of nanoscale materials have promoted an extensive search for methods to prepare highly efficient nanostructured catalysts for the removal of chemical contaminants and harmful gases such as sulfur dioxide and carbon monoxide [1–8]. CO oxidation is a serious environmental concern, since small exposure (ppm) to this odorless invisible gas can be lethal [9]. Therefore, there is a need to develop highly active CO oxidation catalysts to remove even a small amount of CO from the local environment.

In this communication, we report the vapor phase synthesis and characterization of supported Pd, Au and unsupported bimetallic Pd–Au nanoparticle catalysts and compare their catalytic activities for CO oxidation. The approach utilized in the present work is based on the laser vaporization/controlled condensation (LVCC) technique which uniquely combines the features of pulsed laser vaporization of mixed targets prepared from micron-sized commercial metal and metal oxide powders with the controlled condensation process from the vapor phase under well-defined conditions of temperature and pressure [10–12]. The method does not involve the use of any chemical precursors or solvents and therefore, it provides a simple and yet effective synthetic route for supported and unsupported contamination-free, crystalline nanoparticle catalysts.

In the current experiments, commercial micron sized powders are used to prepare compressed pellet targets of selected compositions of the catalyst/support (Pd/S or Au/S), where $S = SiO_2$, ZrO_2 and CeO_2 with known compositions. The target of interest is placed on the lower plate of a diffusion cloud chamber (DCC), and the chamber is filled with He (99.99%) carrier gas. The target is vaporized using the second harmonic generation (532 nm) of a Nd-YAG laser (30–50 mJ/pulse, 10^{-8} s pulse). The temperature gradient between the lower and top plates of the DCC results in a steady convective current which helps to rapidly remove the nanoparticles from the vaporization zone

* Corresponding author. Tel.: +1 804 8283518; fax: +1 804 8288599.
E-mail address: selshall@hsc.vcu.edu (M.S. El-Shall).

1566-7367/$ - see front matter © 2005 Elsevier B.V. All rights reserved.
doi:10.1016/j.catcom.2005.11.014

before they grow into larger particles. The resulting nanoparticles deposited on the cold top plate of the DCC consist of small Pd or Au nanoparticles (5–10 nm) homogeneously dispersed on the surfaces of larger nanoparticle oxide supports such as CeO_2 (40–60 nm) as shown in the TEM images in Fig. 1.

The percent conversions for the CO oxidation are measured using a flow tube reactor coupled to a quadrupole mass spectrometer or an IR detector for the analysis of the gaseous reactants and products (Supporting Information).

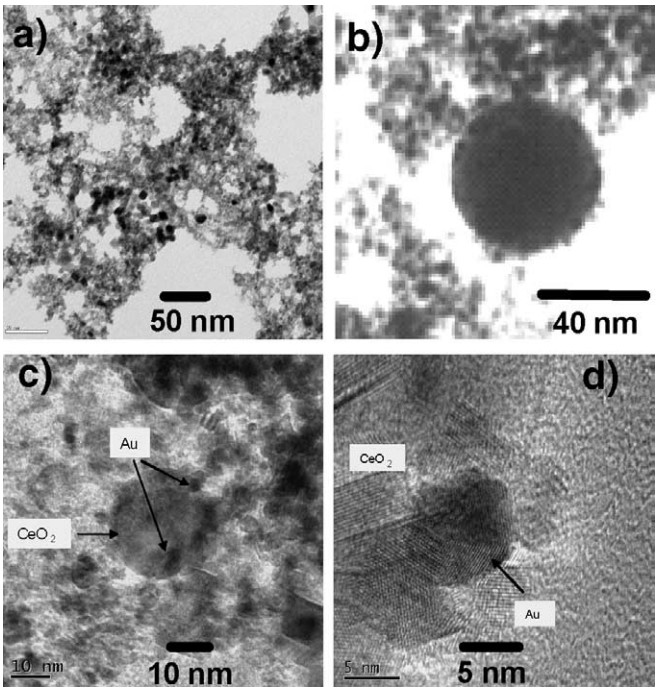

Fig. 1. TEM images of Pd/CeO_2 (a, b), and Au/CeO_2 (c, d) nanoparticle catalysts prepared by the LVCC method.

Fig. 2a compares the CO conversions of the as-prepared 5% Pd/CeO_2 with pure Pd and CeO_2 nanoparticles. Fig. 2b compares the conversions of the as-prepared 5% Au/CeO_2 with a physical mixture consisting of 5% pure Au and 95% pure CeO_2 nanoparticles. In all cases the individual Pd, Au and CeO_2 nanoparticles exhibit higher activities as compared to the corresponding micron-sized particles. This is expected because of the high surface area and more densely populated unsaturated surface coordination sites available in the nanoparticles. However, the very different conversion of the physical mixture of 5% Pd (Au) and 95% CeO_2 nanoparticles from that of the as-prepared 5% Pd/CeO_2 (Au/CeO_2) nanoparticles clearly indicates that laser vaporization of the mixed Pd/CeO_2 (Au/CeO_2) target under the appropriate LVCC conditions can produce Pd (Au) nanoparticles supported on CeO_2 nanoparticles with significant metal–support interaction as shown in Fig. 1. The poor activities of the pure Au nanoparticles and of the $Au + CeO_2$ physical mixture are attributed to the agglomeration of the Au nanoparticles as a result of heating. This effect results in the poor activity of the $Au + CeO_2$ mixture as compared to pure CeO_2 nanoparticles as shown in Fig. 2.

Fig. 3 compares the catalytic conversions of nanoparticle catalysts containing 5% Pd supported on CeO_2, ZrO_2, and SiO_2. The 5% supported Pd/CeO_2 nanoparticles show a CO to CO_2 conversion of 3% at 38 °C, 50% at 82 °C, and a 100% conversion at 108 °C. For comparison, a mixture of 5% micron-sized Pd and 95% micron-sized CeO_2 reaches a maximum conversion of only 90% at temperatures near 300 °C.

The high conversions of the Pd/CeO_2 and Au/CeO_2 nanoparticle catalysts are attributed to the strong interaction between Pd or Au and CeO_2 and to the oxygen storage capacity and redox properties of CeO_2 nanoparticles [13,14]. Our results also indicate that the Pd/CeO_2 and Au/CeO_2 nanoparticle catalysts exhibit excellent stability

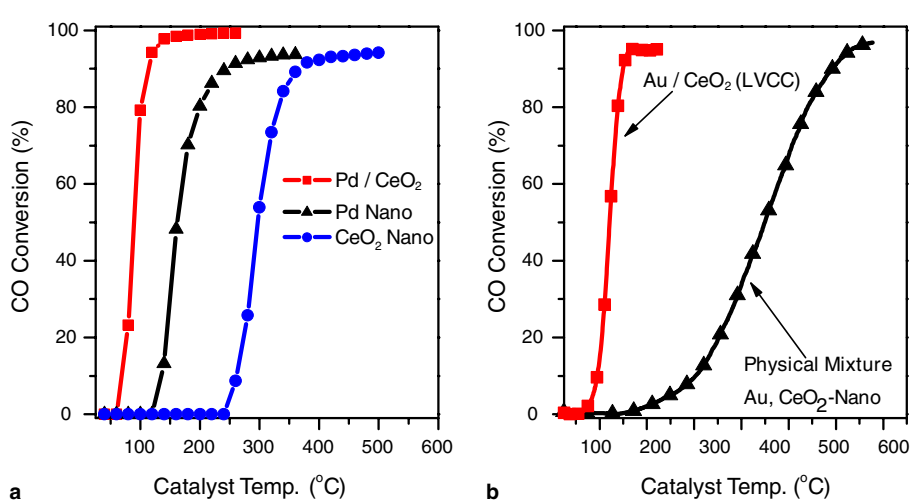

Fig. 2. CO oxidation as a function of temperature for the reactant gas mixture containing 4.0 wt% CO and 20.0 wt% O_2 in helium (20 mg catalyst, flow rate = 100 cc/min).

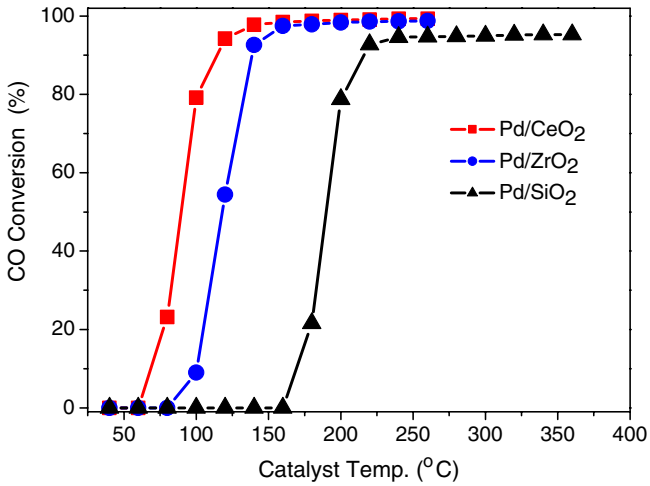

Fig. 3. CO oxidation as a function of temperature for the nanoparticle catalysts of 5% Pd-supported on CeO_2, ZrO_2 and SiO_2 (the reactant gas mixture consists of 4.0 wt% CO and 20.0 wt% O_2 in helium, 20 mg catalyst, flow rate = 100 cc/min).

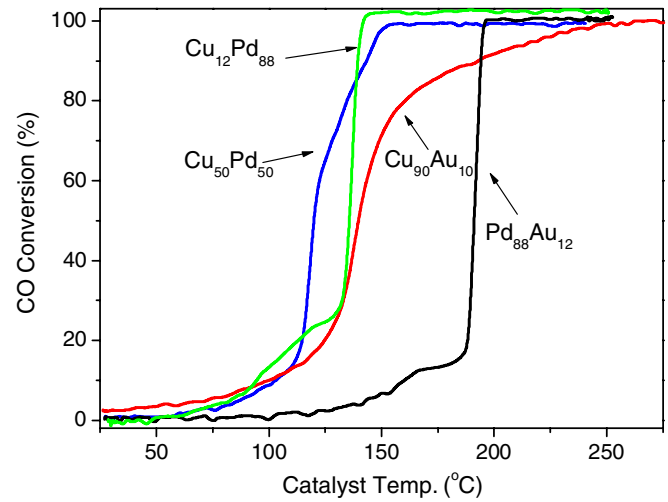

Fig. 4. CO oxidation as a function of temperature for the unsupported bimetallic nanoparticle catalysts.

and reproducibility under typical reaction conditions. For example, at 163 °C the 100% conversion of the Au/CeO_2 nanoparticle catalyst was constant over a test period of 20 h under the flow of the reaction mixture. This stability appears to be one of the most important advantages of using vapor phase synthesis of nanoparticle catalysts due to the elimination of chemical precursors and organic solvents.

Several unsupported bimetallic nanoparticles such as Pd_xAu_{1-x}, Pd_xCu_{1-x}, Au_xCu_{1-x} and Au_xAg_{1-x} with controlled compositions have been prepared by the LVCC method from mixed metal targets and the elemental composition of the resulting alloy nanoparticles have been determined using the ICP technique. Although the composition of the nanoparticles is different from the composition of the bulk mixed target, there is a systematic correlation between the two compositions. For example in the Au_xAg_{1-x} system, for the target metal powder mixtures containing 51.8, 35.6 and 21.2 mol% Au, there are 47.3, 28.7 and 16.6 mol% Au, respectively, in the nanoparticles as determined by the ICP analyses. The XRD diffraction patterns of the bimetallic nanoparticles (Supporting Information) confirm the formation of an alloy in the vapor phase without any indication of the presence of its starting materials.

The CO conversions over several bimetallic nanoparticles measured using an IR gas analyzer, shown in Fig. 4, reveals some interesting observations. First, the activity of the unsupported bimetallic nanoparticles can be tuned to the desired performance depending on the composition of the catalyst. For example, the 3%, 50% and 100% CO conversions occur at the temperatures of 38, 119 and 145 °C for the bimetallic $Cu_{0.90}Au_{0.10}$, $Cu_{0.50}Pd_{0.50}$ and $Cu_{0.12}Pd_{0.88}$ nanoparticle catalysts (as-prepared target compositions), respectively. These are significantly lower temperatures as compared to the bimetallic PdAu nanoparticles supported on TiO_2 where the 1% and 100% CO conversions occur at 150 and 250°C, respectively [8]. Another important finding is obtained from the XRD data taken after the catalysis reaction which indicates the formation of CuO within the bimetallic nanoparticles (Supporting Information). Therefore, the improved conversion efficiencies of these nanoparticles after the catalysis test are attributed to the formation of CuO which is known to have a higher catalytic activity than Cu for CO oxidation [15,16].

Finally, the high activity and stability of the nanoparticle catalysts prepared using the LVCC method are remarkable and imply that a variety of efficient catalysts can be designed and tested using this approach. The significance of the current method lies mainly in its simplicity, flexibility and the control of the different factors that determine the activity of the nanoparticle catalysts. For example, control of the composition of the active metal (Pd, Au, Cu) and the oxide support (CeO_2, ZrO_2, TiO_2, Al_2O_3, and SiO_2) can be achieved by controlling the compositions of the initial targets. Nonstoichiometric oxide supports can be prepared by using metal powders such as Ce, Zr, Ti, Al and Si in the selected targets and carrying out the LVCC process in the presence of varying concentrations of oxygen/helium carrier gas mixtures. Control of the size distribution of the nanoparticle catalysts is accomplished by controlling the pressure of the carrier gas and the temperature gradients during the LVCC synthesis. Size selection is possible through the coupling of the LVCC method with a differential mobility analyzer. The method allows the incorporation of one or more type of active metals such as Pd, Pt, Au, and Cu, or bimetallic alloys such as CuAu, PdAu and CuPd as well as one or more type of oxide supports.

Acknowledgments

We thank Philip Morris USA and NASA (NNG04GH45G) for financial support of this research.

Appendix A. Supplementary data

Figures showing the experimental set up for CO oxidation and the XRD data of the bimetallic catalysts Pd_xAu_{1-x} and Au_xCu_{1-x}. Supplementary data associated with this article can be found, in the online version, at doi:10.1016/j.catcom.2005.11.014.

References

[1] M. Haruta, N. Yamada, T. Kobayashi, S. Iijima, J. Catal. 115 (1989) 301.
[2] W.R. Moser (Ed.), Advanced Catalysts and Nanostructured Materials, Academic Press, 1996.
[3] X. Xu, D.W. Goodman, J. Phys. Chem. 97 (1993) 7711–7718.
[4] M. Valden, X. Lai, D.W. Goodman, Science 281 (1998) 1647–1650.
[5] K.R. McCrea, J.S. Parker, G.A. Somorjai, J. Phys. Chem. B 106 (2002) 10854–10863.
[6] R.W.J. Scott, A.K. Datye, R.M. Crooks, J. Am. Chem. Soc. 125 (2003) 3708–3709.
[7] R.W.J. Scott, O.M. Wilson, S.-K. Oh, E.A. Kenik, R.M. Crooks, J. Am. Chem. Soc. 126 (2004) 15583–15591.
[8] R.W.J. Scott, C. Sivadinarayana, O.M. Wilson, Z. Yan, D.W. Goodman, R.M. Crooks, J. Am. Chem. Soc. 127 (2005) 1380–1381.
[9] World Health Organization, Carbon monoxide, Environmental Health Criteria 213, World Health Organization, Geneva, 1999.
[10] M.S. El-Shall, W. Slack, W. Vann, D. Kane, D. Hanley, J. Phys. Chem. 52 (1994) 3067–3070.
[11] M.S. El-Shall, S. Li, D. Graiver, U.C. Pernisz, in: G. Chow, K.E. Gonsalves (Eds.), Nanotechnology: Molecularly Designed Nanostructural Materials. ACS Symposium Series, vol. 622, 1996, pp. 79–99.
[12] M.S. El-Shall, V. Abdelsayed, Y.B. Pithawalla, E. Alsharach, S.C. Deevi, J. Phys. Chem. B 107 (2003) 2882–2886.
[13] M. Fernandez-Garcia, A. Martinez-Arias, L.N. Salamanca, J.M. Coronado, J.A. Anderson, J.C. Conesa, J. Soria, J. Catal. 187 (1999) 474–486.
[14] Q. Fu, A. Weber, M. Flytzani-Stephanopoulos, Catal. Lett. 77 (2001) 1–3.
[15] J. Wang, De-Hao Tsai, Ta-Jen Huang, J. Catal. 208 (2002) 370–380.
[16] B. Skarman, D. Grandjean, R.E. Benfield, A. Hinz, A. Andersson, L.R. Wallenberg, J. Catal. 211 (2002) 119–133.